Atmospheric Chemistry and Physics

Impact of H_2SO_4/H_2O coating and ice crystal size on radiative properties of sub-visible cirrus

P. Räisänen[1], A. Bogdan[2], K. Sassen[3], M. Kulmala[2], and M. J. Molina[4]

[1]Finnish Meteorological Institute, P.O. Box 503, Helsinki, Finland
[2]Department of Physical Sciences, P.O. Box 64, 00014 University of Helsinki, Finland
[3]Geophysical Institute, University of Alaska, P.O. Box 757320, Fairbanks, AK 99775-7320, USA
[4]Department of Chemistry and Biochemistry, University of California, San Diego, La Jolla, CA 92093-0356, USA

Abstract. Recent laboratory experiments showed that at conditions resembling those near the tropopause region, small ice particles can be coated by a liquid H_2SO_4/H_2O over-layer formed after the freezing of diluted sulfuric acid/water aerosol drops. Here, idealized radiative transfer tests are conducted to evaluate the impact that such an over-layer would have on the radiative effects produced by sub-visible cirrus clouds (SVCs). Spherical particle shape is assumed to keep the problem tractable. The calculations show that the over-layer increases both the shortwave (SW) and longwave (LW) cloud radiative effects (CRE), but the impact is small: $\sim 0.02\,\mathrm{W\,m^{-2}}$, or even less, for the total (LW+SW) CRE at the top of the atmosphere. For the smallest ice particles, for which the over-layer is thickest, the fractional change in CRE can, however, reach $\sim 20\%$ for the SW CRE and over 50% for the LW CRE. The dependence of LW and SW CRE on particle size is also studied in the paper. Calculations for spherical and spheroidal uncoated ice particles show that even for high, optically thin cirrus, the total CRE can be negative, if the diameter of the particles is smaller than about 3–4 μm. Apart from the SVCs, this result could be relevant for contrail cirrus clouds, which are believed to consist of large numbers of very small ice particles.

1 Introduction

Thin high-altitude cirrus clouds with geometrical and optical thickness smaller than 1 km and 0.03, respectively, have obtained an increasing attention due to their potential impact on Earth's climate. These clouds are called sub-visible cirrus clouds (SVCs) because they are invisible for the unaided eye (Sassen and Cho, 1992). Satellite occultation and lidar observations indicate that SVCs are widespread near the tropical and midlatitude tropopause, with a larger frequency of occurrence in the tropics ($\sim 45\%$) than in the midlatitudes (up to 20%) (Wang et al., 1996; Winker and Trepte, 1998). Because of their large areal coverage, especially in the tropics, the SVCs may have a potential effect on climate through reflection of incoming shortwave (SW, solar) radiation and trapping of outgoing longwave (LW, terrestrial) radiation. The SW "albedo" effect brings about cooling and the LW "greenhouse" effect warming of the Earth-atmosphere system. However, as for cirrus clouds in general, the size of the LW and SW effects, and even which of them dominates, can depend on a number of factors in addition to the frequency of SVC occurrence: ice water content, size, shape, orientation and surface properties of ice cloud particles (e.g. Stephens et al., 1990; Sassen, 2002). It has been recognized that the SVCs can also contribute to the destruction of ozone (Solomon et al., 1997; Roumeau et al., 2000; Borrmann et al., 1997; Bregman et al., 2002) which is an important greenhouse gas at high altitudes. Similar to radiative properties, the rate of chlorine activation and concomitant ozone loss depend on microphysical characteristics of the SVCs.

A major uncertainty in the estimates of the climatic impact of the SVCs is a poor knowledge of their microphysics. Microphysical characteristics of the SVCs have been inferred mainly from ground-based (Sassen et al., 1989), airborne (Smith et al., 1998) and satellite-based remote sensing observations (Wang et al., 1996). Direct in situ measurements of microphysical parameters of the SVC ice particles are rather scarce (Heymsfield, 1986; Thomas et al., 2002). Estimates for the SVC microphysical characteristics vary considerably. For example, values derived for the effective diameter of ice particles in the SVCs range from less than 2 μm (Wang et al., 1995) to over 20 μm (McFarquhar et al., 2000), reflecting either substantial variations in the properties of SVCs, or substantial measurement uncertainties, or both.

Correspondence to: P. Räisänen
(petri.raisanen@fmi.fi)

The formation mechanisms of SVCs are also not fully understood yet. Two basic routes of the SVC formation have been described (Jensen at al., 1996). Apparently, some of the SVCs are directly related to deep convection, being essentially the final phase of decaying anvil clouds. However, in other cases, the SVCs are believed to be formed in situ by freezing of diluted sulfuric acid (H_2SO_4/H_2O) aerosol drops of concentration smaller than 30 wt% H_2SO_4 in the presence of slow synoptic-scale uplift (Jensen at al., 1996), which can be provided by tropical waves (Boehm and Verlinde, 2000). Such diluted drops are believed to form by dilution of concentrated H_2SO_4/H_2O aerosol drops that enter the upper troposphere from the lowermost stratosphere through tropopause folds and sedimentation (Hoffman and Rosen, 1983; McCormick et al., 1995; Sassen et al., 1995).

At the most basic level, microphysical properties of cirrus clouds, including the SVCs, are determined by physico-chemical processes occurring at the sub-micrometer to micrometer scales. Neither in situ aircraft measurements nor remote sensing methods can provide direct information on such small-scale processes. Therefore, relevant laboratory studies could be of great importance for better understanding microphysics of young cloud ice particles.

Recently, Bogdan et al. (2004, 2006) have performed laboratory experiments which are of direct relevance to the second SVC formation mechanism mentioned above. Using a differential scanning calorimeter (DSC), they studied the freezing/melting behaviour of emulsified H_2SO_4/H_2O aerosol drops with size and composition resembling those found in the uppermost troposphere. The results (e.g., Fig. 1 in Bogdan et al., 2006) indicated the presence of mixed-phase particles (ice core covered by a H_2SO_4/H_2O over-layer) in temperatures occurring near the tropopause (190–210 K). This supports the speculations by Sassen et al. (1998), who suggested the existence of such particles based on remote and in-situ measurements of very cold corona-producing midlatitude cirrus. The over-layer is thickest for young freshly formed ice particles and becomes thinner as they grow due to water vapor deposition. However, according to our calculations, even ice particles with diameter as large as 5 μm can be coated with an over-layer that is several tens of nanometers thick, depending on the size and initial concentration of the mother H_2SO_4/H_2O aerosol drops.

While it is still unknown how large fraction of SVC clouds actually consist of ice crystals coated by H_2SO_4/H_2O, it is worth studying how such an over-layer would modify the radiative properties of the SVCs. This issue is addressed in Sects. 2 and 3. In addition, we consider in Sect. 4 the impact of ice crystal size on the strength of SVC greenhouse vs. albedo effects, with an extension to contrails.

2 Calculations

2.1 Assumptions about particle composition

Based on the experimental results by Bogdan et al. (2004, 2006) we consider the following scenario for the formation of SVC ice particles (see also Fig. 1):

– *Initial phase*: Ice crystals are initiated by freezing of diluted H_2SO_4/H_2O aerosol drops of diameter $\lesssim 2 \mu$m and composition smaller than 30 wt% H_2SO_4. According to the experimental data, the drop freezing results in the formation of mixed-phase particles: an ice core coated by a H_2SO_4/H_2O over-layer of initial composition of 38 wt% H_2SO_4 (i.e., the composition of the first eutectic point) (Fig. 1a–b).

– *Growth phase*: After the formation, the ice core gradually grows due to deposition of water vapour onto the over-layer and subsequent diffusion of H_2O molecules through it to the ice core. The ice growth will result in formation of thinner and more diluted over-layer because the over-layer volume is limited by the sulfuric acid content. In order to remain liquid, the aged over-layer should have higher H_2SO_4 concentration than that of the mother aerosol drop at the moment of freezing. We assume that the aged over-layer has composition of $\sim$25 wt% H_2SO_4 (Figs. 1c–d).

In-situ observations in SVCs show a variety of ice crystal habits. Heymsfield (1986) reported that the crystals were usually non-spherical, with a 50% mixture of trigonal plates and columns, and that especially the smaller plates had aspect ratios (thickness/diameter) close to 1. On the other hand, recent observations of tropical SVCs by Thomas et al. (2002) indicated that the majority of the ice crystals possessed quasi-spherical shape. The observations by Sassen et al. (1998) in a very cold, although visible, midlatitude cirrus are also relevant here. Most particles were non-spherical, resembling simple plates and columns, but lacking sharp edges and facets that such particles usually have, possibly because particle shapes were influenced by sulfuric acid contamination.

McFarquhar et al. (2000) assessed fairly comprehensively the radiative effects of SVC clouds consisting of pure (i.e., uncoated) ice crystals, assuming non-spherical particle shapes. The H_2SO_4/H_2O over-layer, however, complicates the situation. We are not aware of any computer code suitable for providing the single-scattering properties of coated non-spherical particles for the range of particle size, wavelength and refractive index considered in this study. Therefore, spherical particles are assumed here. While this assumption is not fully realistic, it is unlikely to lead to a qualitatively misleading view of the impact of coating.

For illustrative purposes we consider two cases, Case 1 and Case 2, in which two drops, right before freezing, have the same initial composition of c_0=20 wt% H_2SO_4 but different
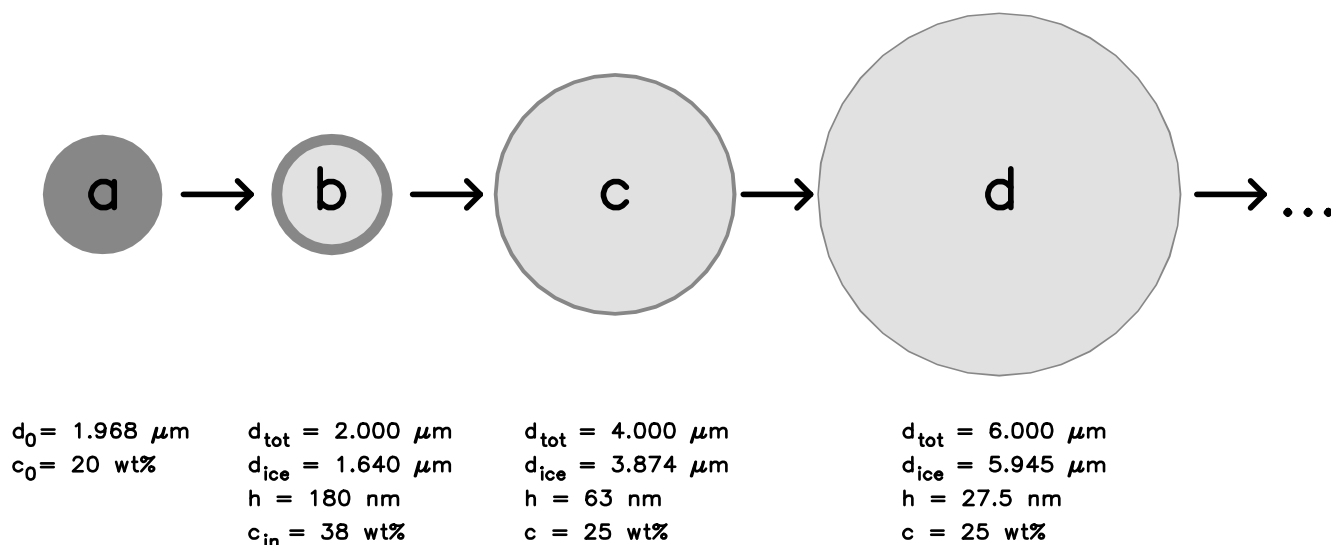
$d_0 = 1.968\ \mu m$ $d_{tot} = 2.000\ \mu m$ $d_{tot} = 4.000\ \mu m$ $d_{tot} = 6.000\ \mu m$
$c_0 = 20\ wt\%$ $d_{ice} = 1.640\ \mu m$ $d_{ice} = 3.874\ \mu m$ $d_{ice} = 5.945\ \mu m$
    $h = 180\ nm$ $h = 63\ nm$ $h = 27.5\ nm$
    $c_{in} = 38\ wt\%$ $c = 25\ wt\%$ $c = 25\ wt\%$

Fig. 1. Simplified illustration of the formation and growth of ice particles in SVC clouds, with numerical values for Case 2. Notation: d_0 and c_0 are initial diameter and composition of the mother drop before freezing, d_{tot} total diameter of the mixed-phase particle (ice core + over-layer), d_{ice} diameter of the ice core, h thickness of the H_2SO_4/H_2O over-layer, c_{in} initial over-layer composition, and c composition in the aged over-layer.

diameters, d_0=0.984 μm and d_0=1.968 μm. These initial diameters are chosen in order to obtain, after freezing, total diameters of the mixed-phase particles equal to d_{tot}=1.000 μm and 2.000 μm, respectively. The mass of acid in the mother drops is 1.14×10^{-13} g and 9.10×10^{-13} g per drop. Right after freezing, the initial composition of the over-layer is c_{in}=38 wt% H_2SO_4, and the over-layer thickness is 89 nm (180 nm) for Case 1 (Case 2) (see Table 1). The composition of the aged over-layer is taken to be c=25 wt% H_2SO_4.

2.2 Computation of single-scattering properties

Single-scattering properties of both uncoated ice crystals and crystals coated with an H_2SO_4/H_2O over-layer were computed using the "coated sphere" Mie code of Bohren and Huffman (1983). For ice refractive index, data from Warren (1984) were used. Refractive index of H_2SO_4/H_2O was computed based on Krieger et al. (2000) for wavelengths λ<1.33 μm and Myhre et al. (2003) for λ>1.33 μm. Computed single-scattering parameters for selected cases are illustrated in Fig. 2.

2.3 Radiative transfer calculations

Radiative transfer calculations were performed using the δ-8-stream discrete ordinate method (Stamnes et al., 1988). Optical depths for gaseous absorption (for H_2O, CO_2, O_3, CH_4, N_2O, $CFCl_3$ and CF_2Cl_2) were computed using a correlated-k distribution code (Li and Barker, 2005). Molecular Rayleigh scattering was likewise included, whereas

aerosols were neglected in the present calculations. The sub-visible cirrus cloud was placed in an otherwise cloud-free tropical model atmosphere (McClatchey et al., 1971) between 16.5 and 17 km (i.e., right below the tropopause). The cloud mid-point temperature is 196 K, and, as in all calculations reported in this paper, a relative humidity of 100% with respect to ice is assumed in the cloud layer. For the shortwave results, diurnal averages were computed, assuming a latitude of 0° N, a solar declination of 10°, and a surface albedo of 0.1.

Essentially monodispersive ice crystal size distributions were assumed; a small but non-zero width of the size distribution was used (effective variance 0.0008) to smooth out small-scale details of Mie scattering results. Although this assumption is not very realistic (e.g., Heymsfield, 1986, reports rather wide size distributions in a SVC cloud), it helps to elucidate the role of particle size. Five values of d_{tot} (1.0 μm, 2.0 μm, 4.0 μm, 6.0 μm, and 10.0 μm) are considered in Table 1. The number concentration of ice crystals was fixed at N=0.3 cm^{-3}. This value was chosen so as to keep the cloud sub-visible even for the largest particle size (d_{tot}=10 μm) considered in Table 1. It is somewhat higher than the values of ~0.05–0.10 cm^{-3} suggested by in situ observations (Heymsfield, 1986; Thomas et al., 2002) but below the maximum concentration of 0.5 cm^{-3} predicted by the model of Jensen at al. (1996). Note that for clouds as thin optically as those considered here, the radiative impact scales, to a good approximation, linearly with N.

Table 1. Impact of H_2SO_4/H_2O coating on the radiative effects of sub-visible cirrus clouds. d_{tot} is the total diameter of (coated or pure) ice particles and h is the over-layer thickness. In the two cases in which h is printed in italic font, the over-layer concentration is $c=c_{in}=38$ wt% H_2SO_4; otherwise $c=25$ wt%. "Case 1" and "Case 2" refer to assumptions about the size of the initial H_2SO_4/H_2O drops, see text. τ_{VIS} (τ_{IR}) is cloud optical depth for the spectral band 0.20–0.69 μm (10.2–12.5 μm), given for the case of pure ice particles. SW CRE, LW CRE and TOT CRE are cloud SW, LW and SW+LW radiative effects at the top of the atmosphere. The differences between clouds consisting of coated and pure ice particles (ΔSW CRE, ΔLW CRE and ΔTOT CRE) are given both in absolute and relative terms. See text for more details.

	d_{tot} (μm)	1 .0	2.0	4.0	6.0	10.0
h (nm)	Case 1	*89.0*	32.0	8.0	3.4	1.2
h (nm)	Case 2		*180.0*	63.0	27.5	9.8
τ_{VIS}	pure ice	0.00041	0.00105	0.00423	0.00931	0.0252
τ_{IR}	pure ice	0.00002	0.00019	0.00159	0.00504	0.0193
SW CRE (W m^{-2})	pure ice	−0.011	−0.060	−0.220	−0.425	−0.965
ΔSW CRE (W m^{-2})	Case 1	−0.003	−0.002	0.000	0.000	0.000
ΔSW CRE (W m^{-2})	Case 2		−0.008	−0.006	−0.003	−0.001
ΔSW CRE (%)	Case 1	25	3	0	0	0
ΔSW CRE (%)	Case 2		14	3	1	0
LW CRE (W m^{-2})	pure ice	0.004	0.034	0.298	0.992	3.900
ΔLW CRE (W m^{-2})	Case 1	0.002	0.003	0.003	0.003	0.001
ΔLW CRE (W m^{-2})	Case 2		0.018	0.024	0.025	0.020
ΔLW CRE (%)	Case 1	54	8	1	0	0
ΔLW CRE (%)	Case 2		53	8	3	1
TOT CRE (W m^{-2})	pure ice	−0.007	−0.026	0.078	0.567	2.935
ΔTOT CRE (W m^{-2})	Case 1	−0.001	0.001	0.003	0.003	0.001
ΔTOT CRE (W m^{-2})	Case 2		0.009	0.018	0.021	0.020
ΔTOT CRE (%)	Case 1	10	−4	3	1	0
ΔTOT CRE (%)	Case 2		−35	23	4	1

3 Results

Table 1 compares SW, LW and total (TOT=SW+LW) cloud radiative effects (CRE) for SVC clouds with uncoated (i.e., pure) ice crystals and for those consisting of coated crystals (Cases 1 and 2). The CREs are defined as

$$\text{CRE} = F^{\text{all}-\text{sky}} - F^{\text{clear}-\text{sky}}, \quad (1)$$

where $F^{\text{all}-\text{sky}}$ and $F^{\text{clear}-\text{sky}}$ are net (down−up) radiative fluxes at the top of the atmosphere (TOA) in the presence and absence of the cloud layer, respectively. Note that in all cases, the comparisons are performed between clouds with uncoated and coated crystals with the same total diameter. Thus, the differences in the CRE arise from differences in particle composition rather than size.

The results in Table 1 indicate that the H_2SO_4/H_2O coating on ice crystals increases both the negative SW CRE and the positive LW CRE of the sub-visible cirrus clouds; the change in LW CRE dominating except for the smallest particle size ($d_{tot}=1.0\,\mu$m) considered. However, in absolute terms, the impact of the H_2SO_4/H_2O over-layer is small. For example, for Case 2, the maximum change

in LW CRE is 0.025 Wm^{-2} (for $d_{tot}=6.0\,\mu$m), the largest change in SW CRE being −0.008 W m^{-2} (for $d_{tot}=2.0\,\mu$m). Even these figures should probably be considered as an upper limit rather than as the most likely values, because the crystal number concentration is fairly high and the initial H_2SO_4/H_2O droplets are relatively large. Indeed, the corresponding changes for Case 1 are much smaller.

Still, it may be noted that for the smallest particle sizes considered (i.e., right after ice core freezing) the H_2SO_4/H_2O coating causes a substantial fractional change in CRE ($\sim$20% for SW CRE and over 50% for LW CRE). The enhancement in SW CRE is explained by two factors of roughly equal importance: a slight increase in the extinction coefficient and a slight decrease in the asymmetry parameter (Fig. 2). The enhancement in LW CRE comes from a substantial increase in absorption coefficient, especially between 4 and 10 μm. However, when the ice core grows through deposition of water vapor, the over-layer becomes thinner and its impact on the single-scattering parameters is reduced (being already quite small for $d_{tot}=6.0\,\mu$m in Fig. 2). Consequently, when the particles reach a size of $d_{tot}=10\,\mu$m, which is a typical value for the effective diameter in in situ observations
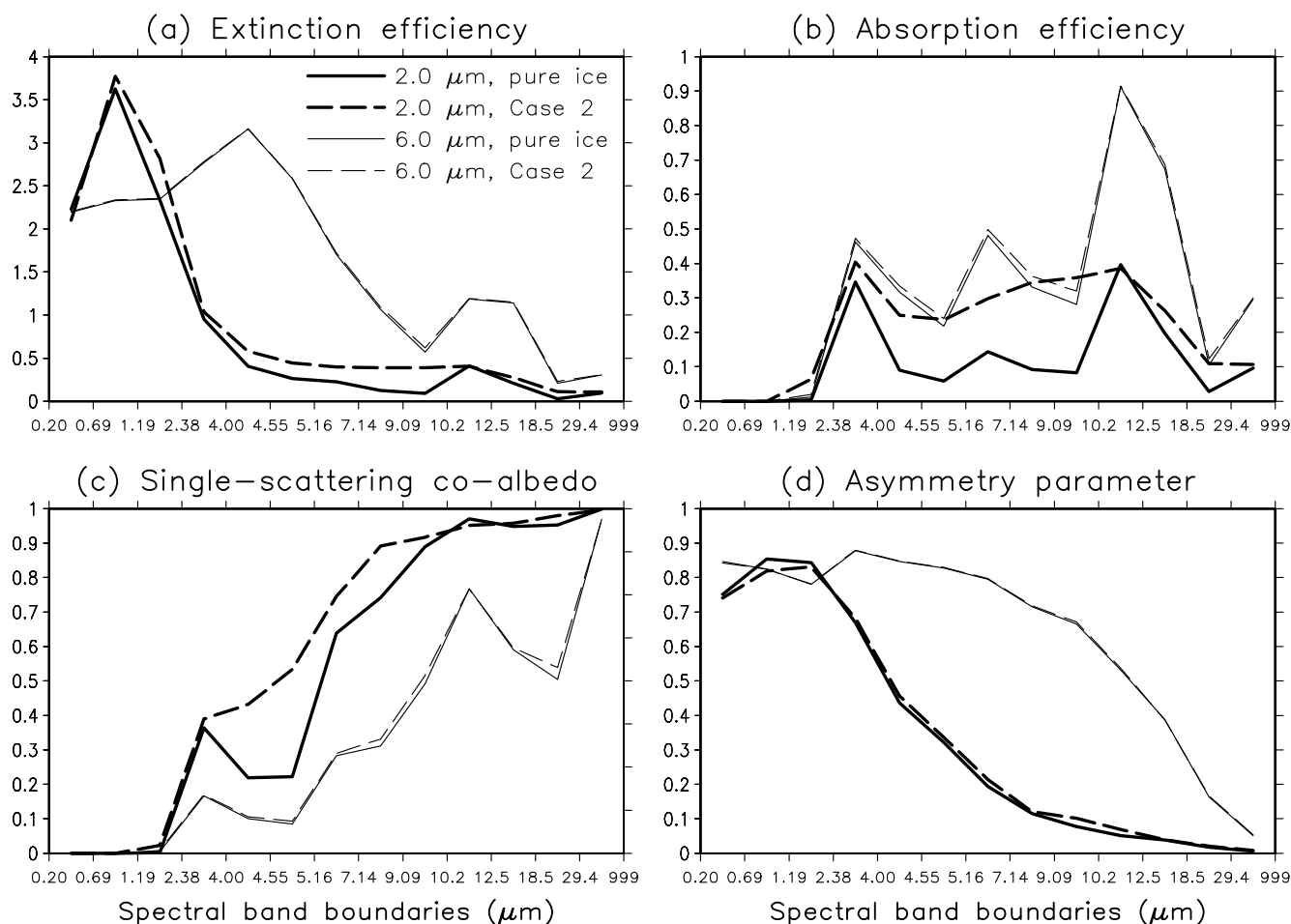
Fig. 2. Single-scattering parameters for pure ice crystals and ice crystals coated with an H_2SO_4/H_2O over-layer (Case 2), for two values of particle diameter (d_{tot}=2.0 μm and d_{tot}=6.0 μm). **(a)** Extinction efficiency Q_{ext} (i.e., ratio of particle extinction cross section to geometrical cross section), **(b)** absorption efficiency Q_{abs}, **(c)** single-scattering co-albedo $1-\varpi=Q_{abs}/Q_{ext}$, and **(d)** asymmetry parameter g. Results are shown for the spectral bands of Li and Barker (2005).

(Heymsfield, 1986; McFarquhar et al., 2000; Thomas et al., 2002), the relative impact of the coating is reduced to 1% or less. Thus, although the coating could produce a substantial fractional change in CRE in the initial phase of the development of SVCs, for mature SVC clouds the impact of coating is most probably small also in a relative sense.

While the direct effect of sulfuric acid coating on the CRE produced by SVC clouds appears small, it may be speculated that indirect effects also exist. In particular, the coating could interfere with water uptake to the ice surface (Sassen et al., 1998), which might help to keep the crystals small for a longer time. If the sublimation and deposition rates are altered, the lifetime of SVC clouds could also be influenced. It seems not unreasonable to suggest that such indirect effects could overwhelm the small direct radiative effects of the coating. Addressing these speculative ideas properly remains, however, beyond the scope of the present study.

Another way in which the coating could, in principle, influence the development of the cloud is through alteration of radiative heating rates in the cloud layer. However, according to our calculations, the maximum difference in total radiative heating rate between Case 2 and the uncoated case was only $\approx$0.025 K d^{-1} (a warming effect) for $d_{tot}\approx$5 μm, which suggests that this mechanism is not important.

4 Impact of particle size on shortwave and longwave cloud radiative effects of thin cirrus

Previous studies on the radiative impacts of sub-visual and thin cirrus have generally reported larger effects on LW than SW radiation (Wang et al., 1996; Smith et al., 1998; McFarquhar et al., 2000), or even neglected the SW effects entirely (Jensen at al., 1999). Our results in Table 1 also indicate that the LW CRE dominates over the SW CRE for the
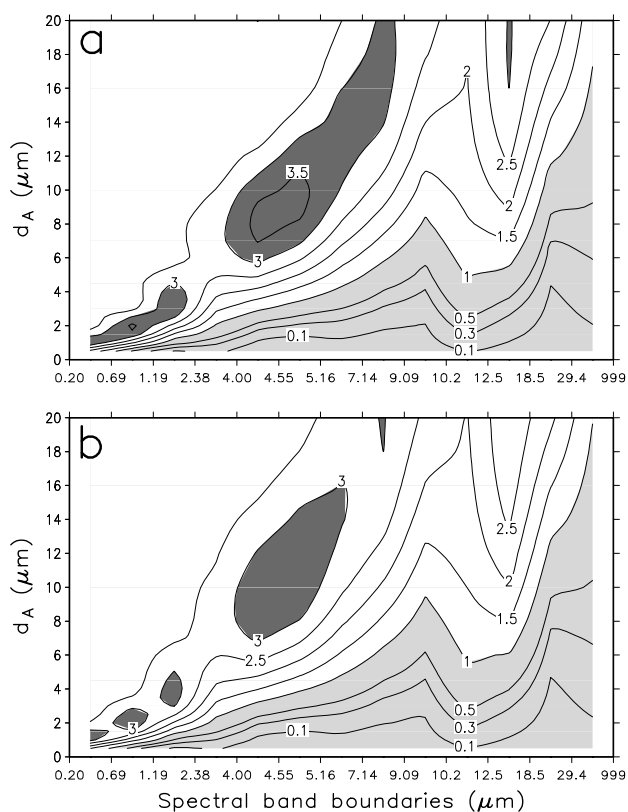
Fig. 3. **(a)** Extinction efficiency Q_{ext} of spherical ice particles as a function of particle size and spectral band. Values above 3 (below 1) are highlighted with dark (light) shading. **(b)** Same as (a), but for a 50/50 mixture of randomly oriented oblate and prolate spheroids with an aspect ratio of 2. d_A is the surface-equivalent particle diameter, which equals the true diameter for spheres. Note the small values of Q_{ext} in the longwave region for small particles.

larger particle sizes ($d_{tot} \geq 4\,\mu m$), which implies that the SVC clouds would have a net warming effect on climate. However, interestingly, the situation is reversed for the smallest particles. For $d_{tot} \leq 2\,\mu m$, the negative SW CRE outweighs the positive LW CRE, although both are very small in absolute terms. This occurs in spite of an extreme temperature difference between the surface (300 K) and the cloud layer (196 K), which would favour the LW CRE.

The relatively small LW CRE for the smallest particle sizes stems from a fact that is as such well-known (e.g. Bohren and Huffman, 1983): for particles very small compared to the wavelength λ, the extinction efficiency (i.e., ratio of extinction cross section to geometrical cross section) is $Q_{ext} \ll 1$. This can be seen in Fig. 2a, and is further illustrated in Fig. 3, which displays Q_{ext} as a function of wavelength and particle size for uncoated ice particles.

For comparison, both spherical and spheroidal ice particles are considered in Fig. 3. For spheroids, an aspect ratio of 2 (i.e., ratio of major to minor axis length) is assumed, with

a 50/50 mixture of oblate and prolate spheroids. The particle size is characterized in terms of the surface-equivalent diameter d_A, which of course equals the true diameter d for spheres. The single-scattering properties of spheroids were computed mainly using the T-matrix method (Mischenko and Travis, 1998), which provided convergent solutions up to size parameters of $x_{max} = \pi d_A / \lambda \sim 70$. For larger sizes, interpolation between the T-matrix results for x_{max} and ray optics results (asymptotically valid for $x \to \infty$) (Muinonen et al., 1996) was used.

Considering first spheres, three regimes can be identified in Fig. 3a. First, in the upper left corner of the plot is the large-particle regime, where Q_{ext} gradually asymptotes toward 2. Second, peaking at $d \sim 2\lambda$, is a regime with somewhat higher values ($Q_{ext} \sim 3$) related to interference between diffracted and transmitted light (Hansen and Travis, 1974). Third, in the lower right part of the plot is the small-particle regime, where Q_{ext} generally decreases with decreasing particle size and increasing wavelength, with some exceptions related to spectral variations of ice refractive index. Consequently, in the LW region, Q_{ext} depends very much on particle size. For very small particles ($d \sim 1\,\mu m$), $Q_{ext} \sim 0.1$, while for relatively "large" particles ($d \gtrsim 15\,\mu m$), $Q_{ext} \gtrsim 2$ in most of the LW region, which is comparable with the values in the SW region. Obviously, this behaviour explains the finding by Khvorostyanov and Sassen (1998) that the ratio of visible to infrared optical thickness increases with decreasing particle size.

For spheroids (Fig. 3b), the behavior of Q_{ext} is very similar to the spherical case, which suggests that the results are not overly sensitive to particle shape. Some differences can be discerned, however. The maximum in Q_{ext} for "midsize" particles is slightly weaker for spheroids than spheres, at least partly due to averaging over different particle orientations and shapes (T. Nousiainen, personal communication). It is also displaced toward slightly larger particle size. Moreover, for smaller size parameters (i.e., almost throughout the LW region), Q_{ext} is consistently slightly lower for spheroids than for spheres with equal surface area. This result is consistent with the analysis by Arnott et al. (1994) based on anomalous diffraction theory. Their Eq. (5) indicates that the absorption efficiency Q_{abs} is directly proportional to the ratio of crystal volume to projected area in the limit of very small crystals. Since the volume-to-area ratio is maximal for spheres, it follows that non-sphericity generally reduces Q_{abs} and Q_{ext}, when the particles are small compared to the wavelength.

The radiative consequences of the size dependence of Q_{ext} (and to a lesser extent, single-scattering co-albedo and scattering phase function) are demonstrated in Fig. 4, both for spherical and spheroidal ice crystals. A cloud located between 16.5 and 17 km in a tropical model atmosphere is again considered in Fig. 4a. However, instead of prescribing particle number concentration N as in Table 1, the total projected area of the ice crystals in the cloud is prescribed as
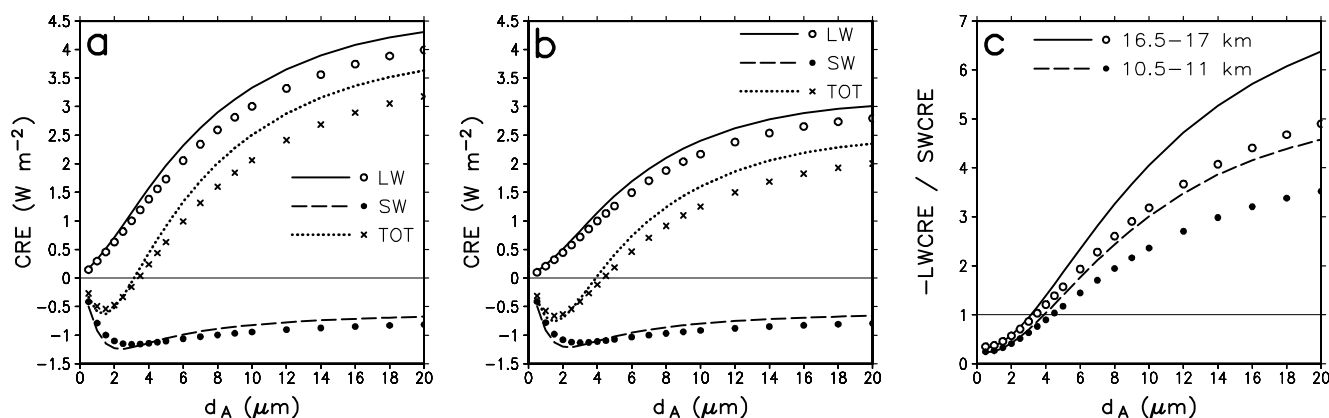
Fig. 4. Longwave (LW), shortwave (SW) and total (TOT) cloud radiative effect (CRE) at the TOA as a function of the surface-equivalent particle diameter d_A for a cloud height of **(a)** 16.5–17 km and **(b)** 10.5–11 km. The lines give results for spherical ice particles, while the symbols represent a 50/50 mixture of randomly oriented oblate and prolate spheroids with an aspect ratio of 2. The ratio of $-$LW CRE/SW CRE is given in **(c)**. The total projected area of the particles is fixed at A_p=0.01 m^2/m^2.

$$A_p = \frac{\pi}{4} d_A^2 N \Delta z = 0.01 \text{ m}^2/\text{m}^2, \qquad (2)$$

where Δz is cloud geometrical thickness. Although this results, for the smallest sizes d_A considered, in unrealistically high N for a cloud near the tropical tropopause, it helps to highlight the impact of variations in Q_{ext}, since the optical thickness is now simply τ=0.01 Q_{ext}.

In accord with the behavior of Q_{ext} in Fig. 3, the LW CRE depends greatly on d_A in Fig. 4a. It is very small for the smallest particles and increases first quasi-linearly, then slower with increasing d_A. In comparison, the SW CRE varies much less with d_A, although a minimum (i.e., largest negative values) can be seen at $d_A \approx$2.5–3 μm, which is also consistent with the variations of Q_{ext} in Fig. 3. Consequently, the ratio of LW CRE to SW CRE (Fig. 4c) depends strongly on particle size. The SW CRE dominates for the smallest particles up to $d_A \approx$3–3.5 μm, whereas for larger particles, the LW CRE dominates, being five to six times as large as the SW CRE for d_A=20 μm.

The impact of small ice particles on the radiative properties of cirrus clouds is an important topic, which can only be resolved properly when better observations of the smallest particles are obtained (Sassen, 2002; Kahn et al., 2003). Typical estimates of effective particle diameter in cirrus clouds are several tens of micrometers (e.g., Table 2 in Fu, 1996), but there are special cases where ice cloud radiative properties may be dominated by much smaller particles. Apart from the SVCs, this could be the case, at least, for aircraft contrails and some orographic clouds (Kahn et al., 2003). Goodman et al. (1998) report effective diameters of $\approx$4 μm in young contrails. Baumgardner and Gandrud (1998) even suggest that most of the condensate is in particles smaller than 1 μm, although many of the numerous very small particles might

actually be unactivated aerosols. The estimates by Liou et al. (1998) for particle size in contrails are slightly higher, with effective mean sizes of 4.9 to 15.9 μm.[1]

Referring to contrails, Fig. 4 also shows results for a cloud located at 10.5–11 km (i.e., at a typical aircraft cruising altitude), the cloud midpoint temperature being 232 K. For this cloud, the LW CRE is smaller than for the near-tropopause cirrus cloud, so the cross-over-point with zero total CRE shifts toward larger particle size, to $d_A \approx$4 μm. This falls in the range of contrail particle sizes quoted above. It is thus possible that in some cases, contrails could actually have a cooling effect on climate.

The possibility of contrails causing cooling was already raised by Khvorostyanov and Sassen (1998). Their calculations for a contrail with mean crystal diameter of $\sim$6 μm indicated slightly positive total CRE at the TOA but distinctly negative total CRE at the surface. They argued that the negative CRE at the surface could lead to local cooling, whereas the positive CRE at the TOA might give rise to warming at larger distances and time scales. Our calculations confirm that the negative SW CRE dominates over the positive LW CRE at the surface. Moreover, this even occurs for relatively large particles. For example, for a cloud height of 10.5–11 km and d_A=20 μm (the largest particle size considered in Fig. 4) the LW CRE at the surface is only 0.23 W m^{-2} (0.22 W m^{-2}) for spheres (spheroids) as compared with a SW CRE of $-$0.55 W m^{-2} ($-$0.67 W m^{-2}). The smallness of the LW CRE results simply from the troposphere being fairly non-transparent in the LW region, which strongly attenuates the impact of high clouds on downwelling LW flux at the surface.

---

[1]For spherical particles, the effective mean size of Liou et al. (1998) equals 2/3 of the effective diameter.

Obviously, the tests presented here are idealized. The results would be modified by inclusion of ice crystal size distributions, other crystal shapes and lower cloud layers. However, this would not alter the conclusion that when the particles are sufficiently small, the negative SW CRE can dominate over the positive LW CRE at the TOA, even for optically thin high clouds.

5 Conclusions

The primary purpose of the present paper has been to assess the impact of a sulfuric acid (H_2SO_4/H_2O) over-layer on the radiative properties of sub-visible cirrus clouds that frequently exist near the tropical and midlatitude tropopause region. The existence of such an over-layer is suggested by the recent laboratory measurements (Bogdan et al., 2004, 2006). Our radiative transfer calculations show that the over-layer increases both the longwave and shortwave cloud radiative effects produced by the SVCs, but in absolute terms, the over-layer impact is small (at most $\sim 0.02\,\mathrm{W\,m^{-2}}$, and possibly much less). However, for the smallest ice particles the fractional change in the CRE is substantial and can reach $\sim 20\%$ for the SW CRE and over 50% for the LW CRE.

Beyond the direct radiative impacts, we speculate that the coating could influence the growth of the ice crystals and perhaps the lifetime of SVC clouds by interfering with water uptake to the ice surface. An assessment of this mechanism is, however, left for future work.

The impact of ice particle size on the radiative effects of optically thin cirrus clouds is revisited. The calculations demonstrate that for very small ice particles (diameters less than 3 or 4 μm), the SW CRE can outweigh the LW CRE at the TOA, which means that such clouds would actually have a cooling effect on climate. This is related to small values of extinction efficiency Q_{ext} for particles small compared to the wavelength. While most ice clouds have substantially larger particles, this finding could be relevant for SVCs and contrails in some cases.

Edited by: C. George

References

Arnott, W. P., Dong, Y., Hallett, J., and Poellot, M. R.: Role of small ice crystals in radiative properties of cirrus: A case study, FIRE II, November 22, 1991, J. Geophys. Res., 99, 1371–1381, 1994.

Baumgardner, D. and Gandrud, B. E.: A comparison of the microphysical and optical properties of particles in an aircraft contrail and mountain wave cloud, Geophys. Res. Lett., 25, 1129–1132, 1998.

Boehm, M. T. and Verlinde, J.: Stratospheric influence on upper tropospheric tropical cirrus, Geophys. Res. Lett., 27, 3209–3212, 2000.

Bogdan, A., Molina, M. J., Molina, L. T., and Kulmala, M.: Formation of a liquid over-layer around ice particles in high cirrus clouds, in: Proc. 16-th Intern. Conf. on Nucleation and Atmos. Sci., Kyoto, pp. 123–126, Kyoto Univ. Press, 2004.

Bogdan, A., Molina, M. J., Sassen, K., and Kulmala, M.: Formation of low-temperature cirrus from H_2SO_4/H_2O aerosol droplets. J. Phys. Chem. A, in press, 2006.

Bohren, C. F. and Huffman, D. R.: Absorption and scattering of light by small particles, John Wiley and Sons, New York, 1983.

Borrmann, S., Solomon, S., Avallone, L., Toohey, D., and Baumgardner, D.: On the occurence of ClO in cirrus clouds and volcanic aerosol in the tropopause region, Geophys. Res. Lett., 24, 2011–2014, 1997.

Bregman, B., Wang, P.-H., and Lelieveld, J.: Chemical ozone loss in the tropopause region on subvisible ice clouds, calculated with a chemistry-transport model, J. Geophys. Res., 107, 4032, doi:10.1029/2001JD000761, 2002.

Fu, Q.: An accurate parameterization of the solar radiative properties of cirrus clouds for climate models, J. Climate, 9, 2058–2082, 1996.

Goodman, J., Pueschel, R. F., Jensen, E. J., Verma, S., Ferry, G. V., Howard, S. D., Kinne, S. A., and Baumgardner, D.: Shape and size of contrail ice particles, Geophys. Res. Lett., 25, 1327–1330, 1998.

Hansen, J. and Travis, L.: Light scattering in planetary atmospheres, Space Sci. Rev., 16, 527–610, 1974.

Heymsfield, A. J.: Ice particles in a cirriform cloud at −83°C and implications for polar stratospheric clouds, J. Atmos. Sci., 43, 851–855, 1986.

Hofmann, D. J. and Rosen, J. M.: Sulfuric acid droplet formation and growth in the stratosphere after the 1982 eruption of El Chichon, Science, 222, 325–327, 1983.

Jensen, E. J., Toon, O. B., Selkirk, H. B., Spinhirne, J. D., and Schoeberl, M. R.: On the formation and persistence of subvisible cirrus clouds near the tropical tropopause, J. Geophys. Res., 101, 21 361–21 375, 1996.

Jensen, E. J., Read, W. G., Mergenthaler, J., Sandor, B. J., Pfister, L., and Tabazadeh, A.: High humidities and subvisible cirrus near the tropical tropopause, Geophys. Res. Lett., 26, 2347–2350, 1999.

Kahn, B. H., Eldering, A., Clough, S. A., Fetzer, E. J., Fishbein, E., Gunson, M. R., Lee, S. Y., Lester, P. F., and Realmuto, V. J.: Near micron-sized cirrus cloud particles in high-resolution infrared spectra: An orographic case study, Geophys. Res. Lett., 30, 1441, doi:10.1029/2003GL016909, 2003.

Khvorostyanov, V. I. and Sassen, K.: Cloud model simulation of a contrail case study: Surface cooling versus upper tropospheric warming, Geophys. Res. Lett., 25, 2145–2148, 1998.

Krieger, U. K., Mössinger, J. C., Luo, B., Weers, U., and Peter, T.: Measurement of the refractive indices of H_2SO_4-HNO_3-H_2O solutions to stratospheric temperatures, Appl. Opt., 39, 3691–3703, 2000.

Li, J. and Barker, H. W.: A radiation algorithm with correlated-*k* distribution. Part I: Local thermal equilibrium, J. Atmos. Sci., 62, 286–309, 2005.

Liou, K. N., Yang, P., Takano, Y., Sassen, K., Charlock, T., and Arnott, W.: On the radiative properties of contrail cirrus, Geophys. Res. Lett., 25, 1161–1164, 1998.

Mishchenko, M. I. and Travis, L. D.: Capabilities and limitations of a current Fortran implementation of the *T*-matrix method for randomly oriented, rotationally symmetric scatterers, J. Quant. Spectrosc. Radiat. Transfer, 60, 309–324, 1998.

McClatchey, R. A., Fenn, R. W., Selby, J. E. A., Volz, F. E., and Garing, J. S.: Optical properties of the atmosphere, Report AFCRL-71-0279 (available from Air Force Geophysics Laboratory, Hanscom Air Force Base, MA 01731, USA), 1971.

McFarquhar, G. M., Heymsfield, A. J., Spinhirne, J., and Hart, B.: Thin and subvisual tropopause tropical cirrus: Observations and radiative impacts, J. Atmos. Sci., 57, 1841–1853, 2000.

McCormick, M. P., Thomason, L. W., and Trepte, C. R.: Atmospheric effects of the Mt Pinatubo eruption, Nature, 373, 399–404, 1995.

Muinonen, K., Nousiainen, T., Fast, P., Lumme, K., and Peltoniemi, J. I.: Light scattering by Gaussian random particles: Ray optics approximation, J. Quant. Spectrosc. Radiat. Transfer, 55, 577–601, 1996.

Myhre, C. E. L., Christensen, D. H., Nicolaisen, F. M., and Nielsen, C. J.: Spectroscopic study of aqueous H_2SO_4 at different temperatures and compositions: Variations in dissociation and optical properties, J. Phys. Chem. A, 107, 1979–1991, 2003.

Roumeau, S., Bremaud, P., Rviere, E., Baldy, S., and Baray, J. L.: Tropical cirrus clouds: a possible sink for ozone, Geophys. Res. Lett., 27, 2233–2236, 2000.

Sassen, K.: Cirrus clouds: A modern perspective, in: Cirrus, edited by: Lynch, D. K., Sassen, K., Starr, D. O'C., and Stephens, G. L., pp. 11–40, Oxford Press, New York, 2002.

Sassen, K. and Cho, B. S.: Subvisual-thin cirrus lidar dataset for satellite verification and climatological research, J. Appl. Meteor., 31, 1275–1285, 1992.

Sassen, K., Griffin, M. K., and Dodd, G. C.: Optical scattering and microphysical properties of subvisible cirrus clouds, and climatic implications, J. Appl. Meteor., 28, 91–98, 1989.

Sassen, K., Starr, D. O'C., Mace, G. G., Poellot, M. R., Melfi, S. H., Eberhard, W. L., Spinhirne, J. D., Eloranta, E. W., Hagen, D. E., and Hallett, J.: The 5–6 December 1991 FIRE IFO II jet stream cirrus case study: Possible influences of volcanic aerosols, J. Atmos. Sci., 52, 97–123, 1995.

Sassen, K., Mace, G. G., Hallett, J., and Poellot, M. R.: Corona-producing ice clouds: a case study of a cold mid-latitude cirrus layer, Appl. Opt., 37, 1477–1485, 1998.

Smith, W. L., Ackerman, S., Revercomb, H., Huang, H., DeSlover, D. H., Feltz, W., Gumley, L., and Collard, A.: Infrared spectral absorption of nearly invisible cirrus clouds, Geophys. Res. Lett., 25, 1137–1140, 1998.

Solomon, S., Borrman, S., Garcia, R. R., Portmann, R., Thomason, L., Poole, L. R., Winker, D., and McCormick, M. P.: Heterogeneous chlorine chemistry in the tropopause region, J. Geophys. Res., 102, 21 411–21 429, 1997.

Stamnes, K., Tsay, S.-C., Wiscombe, W., and Jayaweera, K.: Numerically stable algorithm for discrete-ordinate-method radiative transfer in multiple scattering and emitting layered media, Appl. Opt., 27, 2502–2509, 1988.

Stephens, G. L., Tsay, S.-C., Stackhouse Jr., P. W., and Flatau, P. J.: The relevance of the microphysical and radiative properties of cirrus clouds to climate and climatic feedback, J. Atmos. Sci., 47, 1742–1753, 1990.

Thomas, A., Borrman, S., Kiemle, C., Cairo, F., Volk, M., Beuermann, J., Lepuchov, B., Santacesaria, V., Matthey, R., Rudakov, V., Yushkov, V., McKenzie, A. R., and Stefanutti, L.: In situ measurements of background aerosol and subvisible cirrus in the tropical tropopause region, J. Geophys. Res., 107, 4763, doi:10.1029/2001JD001385, 2002.

Wang, P.-H., Minnis, P., and Yue, G. K.: Extinction coefficient (1 μm) properties of high-altitude clouds from solar occultation measurements (1985–1990): Evidence of volcanic aerosol effect, J. Geophys. Res., 100, 3181–3199, 1995.

Wang, P.-H., Minnis, P., McCormick, M. P., Kent, G. S., and Skeens, K. M.: A 6-year climatology of cloud occurrence frequency from stratospheric aerosol and gas experiment II observations (1985–1990), J. Geophys. Res., 101, 29 407–29 429, 1996.

Warren, S. G.: Optical constants of ice from the ultraviolet to the microwave, Appl. Opt., 23, 1206–1225, 1984.

Winker, D. M. and Trepte, C. R.: Laminar cirrus observed near the tropical tropopause by LITE, Geophys. Res. Lett., 25, 3351–3354, 1998.